AMERICAN SOCIETY FOR MICROBIOLOGY | Molecular and Cellular Biology®

RESEARCH ARTICLE

GATA2 and PU.1 Collaborate To Activate the Expression of the Mouse *Ms4a2* Gene, Encoding FcεRIβ, through Distinct Mechanisms

Shin'ya Ohmori,[a] Yasushi Ishijima,[b] Suzuka Numata,[a] Mai Takahashi,[a] Masataka Sekita,[a] Taichi Sato,[a] Keisuke Chugun,[a] Masayuki Yamamoto,[c] Kinuko Ohneda[a]

[a]Department of Pharmacy, Faculty of Pharmacy, Takasaki University of Health and Welfare, Takasaki, Japan
[b]Department of Pharmaceutical Sciences, Faculty of Pharmaceutical Sciences, Suzuka University of Medical Science, Suzuka, Japan
[c]Department of Medical Biochemistry, Tohoku University Graduate School of Medicine, Miyagi, Japan

ABSTRACT GATA factors GATA1 and GATA2 and ETS factor PU.1 are known to function antagonistically during hematopoietic development. In mouse mast cells, however, these factors are coexpressed and activate the expression of the *Ms4a2* gene encoding the β chain of the high-affinity IgE receptor (FcεRI). The present study showed that these factors cooperatively regulate *Ms4a2* gene expression through distinct mechanisms. Although GATA2 and PU.1 contributed almost equally to *Ms4a2* gene expression, gene ablation experiments revealed that simultaneous knockdown of both factors showed neither a synergistic nor an additive effect. A chromatin immunoprecipitation analysis showed that they shared DNA binding to the +10.4-kbp region downstream of the *Ms4a2* gene with chromatin looping factor LDB1, whereas the proximal −60-bp region was exclusively bound by GATA2 in a mast cell-specific manner. Ablation of PU.1 significantly reduced the level of GATA2 binding to both the +10.4-kbp and −60-bp regions. Surprisingly, the deletion of the +10.4-kbp region by genome editing completely abolished the *Ms4a2* gene expression as well as the cell surface expression of FcεRI. These results suggest that PU.1 and LDB1 play central roles in the formation of active chromatin structure whereas GATA2 directly activates the *Ms4a2* promoter.

KEYWORDS GATA transcription factors, high-affinity IgE receptor, mast cell, transcriptional regulation

The zinc finger transcription factors GATA1 and GATA2 and the ETS family transcription factor PU.1 play essential roles in hematopoietic development. GATA1 is known as a master regulator of erythropoiesis throughout life (1–4), whereas GATA2 plays indispensable roles in the proliferation and survival of immature hematopoietic progenitors (5, 6). PU.1 is encoded by the *SPI1* and *Spi1* genes in humans and mice, respectively, and is necessary for the generation of myeloid and B cells (7, 8). Numerous studies have shown that GATA factors and PU.1 cross-inhibit their respective activities through multiple routes, including repressing the expression, blocking the DNA binding activity, and inhibiting the recruitment of transcriptional coactivators (9–15). These studies provided evidence that the GATA factors and PU.1 are reciprocally expressed, regulate distinct sets of target genes, and thereby function antagonistically during hematopoietic development.

Compared to this functional antagonism, however, much less is known about the cooperative interplay between the GATA factors and PU.1, despite the fact that they are coexpressed in some myeloid cell lineages, such as eosinophils, basophils, and mast cells (MCs). Only a few studies have described cooperative or synergistic, rather than

Citation Ohmori S, Ishijima Y, Numata S, Takahashi M, Sekita M, Sato T, Chugun K, Yamamoto M, Ohneda K. 2019. GATA2 and PU.1 collaborate to activate the expression of the mouse *Ms4a2* gene, encoding FcεRIβ, through distinct mechanisms. Mol Cell Biol 39:e00314-19. https://doi.org/10.1128/MCB.00314-19.

Address correspondence to Kinuko Ohneda, kohneda@megabank.tohoku.ac.jp.

Received 16 July 2019
Returned for modification 16 August 2019
Accepted 2 September 2019
Accepted manuscript posted online 9 September 2019
Published 28 October 2019

antagonistic, gene regulation by the GATA factors and PU.1 in these lineages. For instance, GATA1 and PU.1 synergistically activate the major basic protein P2 promoter in eosinophils (16), and in mast cells and basophils, GATA2 and PU.1 cooperatively activate the human *ST2* gene promoter (17). However, the molecular basis underlying the functional cooperation has not been well elucidated.

We previously examined mast cell-specific gene expression in bone marrow-derived mast cells (BMMCs) prepared from GATA1 (18) or GATA2 (19) conditional knockout (KO) mice. Our data suggested that GATA1 and GATA2 performed overlapping roles by regulating common target genes whereas GATA2 played more important roles than GATA1 in the target gene regulation (18, 19). The β chain of the high-affinity IgE receptor (FcεRIβ), encoded by the *Ms4a2* gene, is a representative target gene regulated by the GATA factors. We showed that the cell surface expression of FcεRI was reduced and the FcεRIβ mRNA level significantly decreased by GATA2 ablation (19). Although these phenotypes were not observed in GATA1 knockout BMMCs, a chromatin immunoprecipitation (ChIP) assay showed that both GATA1 and GATA2 bound to the *Ms4a2* promoter (18). The involvement of the GATA factors in the regulation of the human *MS4A2* and mouse *Ms4a2* genes has been reported in previous studies as well (20–22). Interestingly, a recent study showed that *Ms4a2* gene expression is also affected by small interfering RNA (siRNA)-mediated knockdown (KD) of PU.1 in mouse BMMCs (23). Thus, it is speculated that the mouse *Ms4a2* gene might be regulated cooperatively by the GATA factors and PU.1 in mast cells.

LIM domain-binding protein 1 (LDB1) is a ubiquitously expressed and highly conserved nuclear protein that was originally identified as a partner for the LIM homeodomain or the LIM-only proteins (24; reviewed in reference 25). In erythroid cells, LDB1 interacts with a LIM-only protein (LMO2), GATA1, and SCL/TAL (26), and this protein complex plays a critical role in the formation of the enhancer-promoter loop formation of the *β-globin* and *Myb* genes (27–29). More recently, LDB1 was shown to be required for the self-activation of the *Spi1* gene in myeloid cells (30), while its role in mast cells has been unclear.

FcεRIβ is a component of FcεRI that plays a key role in the IgE-mediated immune response in mast cells. Whereas FcεRIα specifically binds to IgE, the β and γ subunits of FcεRI amplify and transduce intracellular signaling, respectively (31, 32). The *MS4A2* and *Ms4a2* genes are located on chromosomes 11 and 19 in humans and mice, respectively. The expression of the *MS4A2*/*Ms4a2* gene is restricted in mast cells and basophils. In mice, it is required for the trafficking and localization of FcεRI to the cell membrane (33, 34). Human FcεRIβ can promote glycosylation of immature FcεRIα protein and stabilize the cell surface expression of the FcεRI complex (35). Previous studies have shown that single nucleotide polymorphisms (SNPs) in the human *MS4A2* gene are associated with an increased risk of asthma (36) and allergic rhinitis (37). More recently, some SNPs in the *MS4A2* gene were found to be associated with hypersensitivity to nonsteroidal anti-inflammatory drugs (38, 39). Despite its functional and clinical importance, transcriptional regulation of the *MS4A2*/*Ms4a2* gene remains poorly understood.

Since FcεRIβ is a key molecule for mast cell-specific cellular function, clarifying the molecular mechanisms underlying the *Ms4a2* gene regulation might facilitate our understanding of mast cell-specific gene regulation. We are particularly interested in how the antagonistic transcription factors (GATA factors and PU.1) cooperatively regulate a common target gene in mast cells. Thus, the present study explored the roles of GATA factors and PU.1 in the regulation of the *Ms4a2* gene.

RESULTS

Ablation of PU.1 and GATA2 affected Ms4a2 mRNA expression to the same extent. In this study, we prepared BMMCs from *Spi1*$^{flox/flox}$::*Rosa26-CreER*^{T2} (*Spi1*$^{f/f}$::*CreER*^{T2}) and *Gata2*$^{flox/flox}$::*Rosa26CreER*^{T2} (*Gata2*$^{f/f}$::*CreER*^{T2}) mutant mice that had been treated with 4-hydroxytamoxifen (4-OHT) to induce Cre-loxP-mediated recombination (PU.1-KO and GATA2-KO BMMCs, respectively). Consistent with a previous report describing PU.1 KD BMMCs (23), fluorescence-activated cell sorter (FACS) analysis

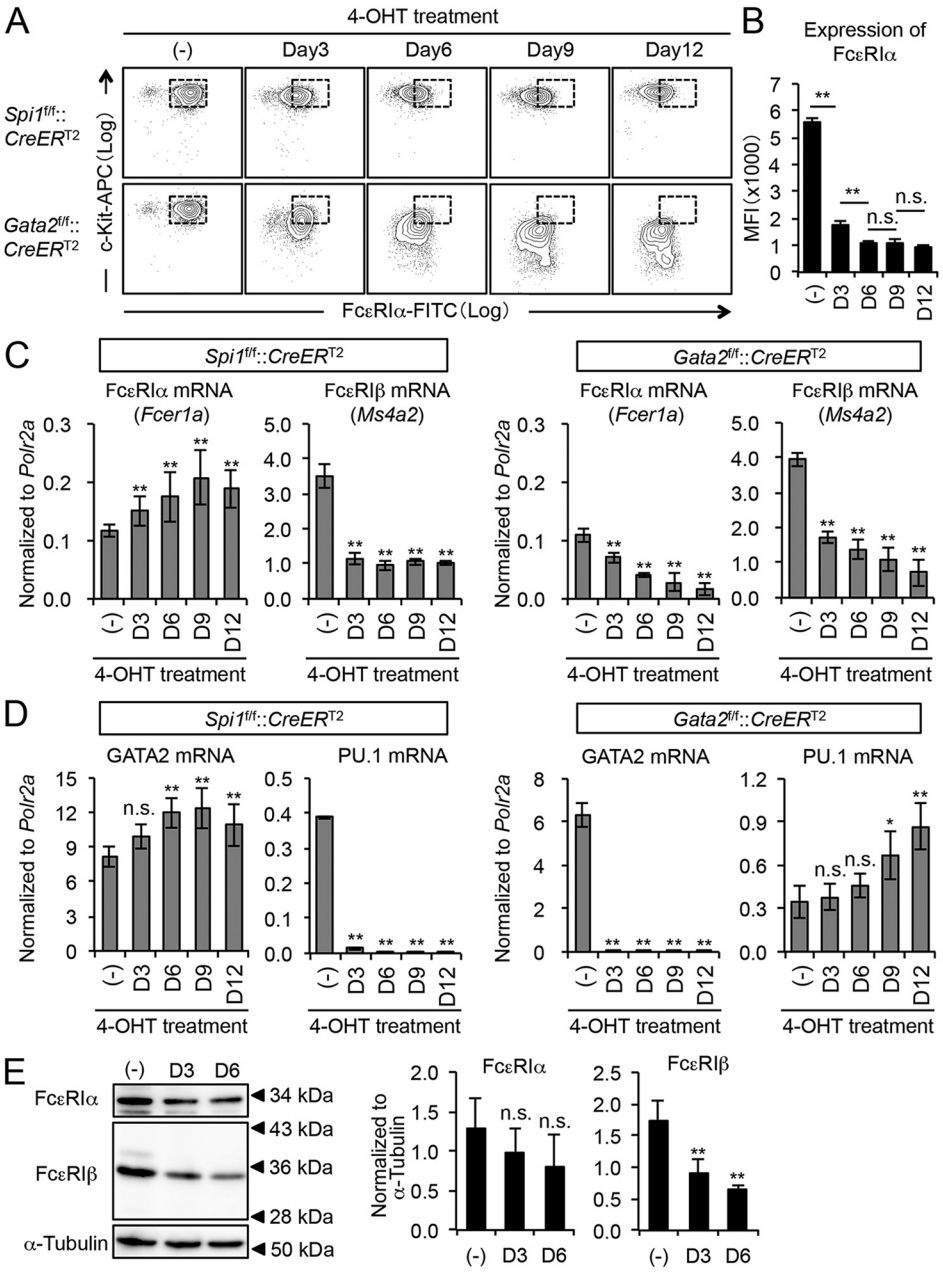

FIG 1 Ablation of PU.1 and GATA2 affected the FcεRIα mRNA expression to the same extent. (A) Representative FACS data for BMMCs prepared from *Spi1*$^{f/f}$::*CreER*^{T2} and *Gata2*$^{f/f}$::*CreER*^{T2} mice after 4-OHT treatment. Data are representative of results from five independent experiments. Samples prepared after 0, 3, 6, 9, and 12 days of 4-OHT treatment are indicated by (-), Day3, Day6, Day9, and Day12, respectively. FITC, fluorescein isothiocyanate. (B) MFI of FcεRIα expression on BMMCs prepared from *Spi1*$^{f/f}$::*CreER*^{T2} mice after 4-OHT treatment. The data were analyzed by one-way ANOVA with Tukey's *post hoc* test. $n = 5$. (C and D) The results of qRT-PCR of the indicated genes in the BMMCs prepared from *Spi1*$^{f/f}$::*CreER*^{T2} (C) or *Gata2*$^{f/f}$::*CreER*^{T2} (D) mice after 0, 3, 6, 9, and 12 days of 4-OHT treatment. $n = 5$. (E) A Western blot analysis and densitometry graphs of FcεRIα, FcεRIβ, and α-tubulin expression. Cytoplasmic extracts were isolated from *Spi1*$^{f/f}$::*CreER*^{T2} BMMCs treated with 4-OHT for 0, 3, and 6 days [(-), D3, and D6, respectively]. α-Tubulin was used as a loading control. Densitometry analysis was performed on the FcεRIα and FcεRIβ blots, and the relative intensities were plotted on the bar graph (right panel). $n = 5$. For panels C, D, and E, the data were analyzed by one-way ANOVA with Dunnett's *post hoc* test and compared to the data for 4-OHT(-). *, $P < 0.05$; **, $P < 0.01$; n.s., not significant.

revealed a decrease in FcεRIα expression that was observed from day 3 on and that did not affect c-Kit expression (Fig. 1A). In contrast, cell surface expression of both c-Kit and FcεRIα was significantly reduced on the GATA2-KO BMMCs (19), as previously reported (Fig. 1A). Notably, the level of FcεRIα expression on the PU.1-KO BMMCs remained low after day 6 (Fig. 1B), indicating that PU.1 partially affected the expression of FcεRI.

We then examined the mRNA levels of FcεRIα and FcεRIβ encoded by the *Fcer1a* and *Ms4a2* genes, respectively, in the PU.1-KO or GATA2-KO BMMCs by quantitative reverse transcription-PCR (qRT-PCR) (Fig. 1C). Despite the level of FcεRIα protein expression on the cell surface being decreased (Fig. 1A), the FcεRIα mRNA levels were increased in the PU.1-KO BMMCs (Fig. 1C). In contrast, the FcεRIβ mRNA levels were decreased and correlated with the FcεRIα expression levels in the FACS analysis. In the GATA2-KO BMMCs, the mRNA levels of both FcεRIα and FcεRIβ were decreased (Fig. 1C). On day 3 of 4-OHT treatment, the PU.1 and GATA2 mRNA levels were significantly reduced in the corresponding knockout BMMCs, suggesting that Cre-loxP-mediated recombination had been completed (Fig. 1D). The GATA2 mRNA level was increased in the PU.1-KO BMMCs and vice versa (Fig. 1D), suggesting that GATA2 and PU.1 each cross-inhibit the expression of the other in BMMCs. The time course expression profile of GATA2 mRNA was similar to that of FcεRIα in the PU.1-KO BMMCs, suggesting that expression of FcεRIα might be dependent on GATA2. Western blotting showed that the FcεRIβ protein level had also been decreased by PU.1 deletion starting from day 3 of 4-OHT treatment (Fig. 1E). Despite the FcεRIα mRNA levels having increased following PU.1 deletion (Fig. 1C), the FcεRIα protein levels were not increased and even showed a trend toward a decrease in the cell lysate (Fig. 1E). Although the molecular basis for the result is unknown, the loss of FcεRIα from the cell surface might have been caused by both the decreased FcεRIα protein levels in the cells and the impaired FcεRIβ-mediated intracellular trafficking of the FcεRI complex.

Simultaneous KD of GATA2 and PU.1 failed to further decrease the expression of FcεRI on MEDMC-BRC6 mast cells. We noted that FcεRIβ mRNA expression was not completely eliminated by conditional knockout of either GATA2 or PU.1 (Fig. 1C) and considered the possibility that the FcεRIβ mRNA level would be further decreased by a reduction in both factors. To simultaneously reduce the levels of GATA2 and PU.1, we introduced siRNAs targeting GATA2 and PU.1 into MEDMC-BRC6 (BRC6) mast cells (40). The mRNA levels of the transcription factors (GATA1, GATA2, and PU.1) of the BMMCs and BRC6 cells were similar, whereas those of mast cell markers (FcεRIα, FcεRIβ, and c-Kit) were lower in BRC6 cells than in BMMCs (Fig. 2A). The results of a FACS analysis performed using the PU.1-KD or GATA2-KD BRC6 cells were consistent with those of analyses of the corresponding KO BMMCs, although the reduction in the level of c-Kit expression was less significant in the GATA2-KD BRC6 cells than in the GATA2-KO BMMCs (Fig. 2B). Unexpectedly, the simultaneous KD of PU.1 and GATA2 in BRC6 cells did not further decrease the FcεRIα level compared to that in the cells transfected with either PU.1 or GATA2 siRNA (Fig. 2B and C). To evaluate the contribution of GATA1 to FcεRI expression, we introduced GATA1 siRNA into BRC6 cells in combination with GATA2 and/or PU.1 siRNAs (Fig. 2B). Expression of FcεRI or c-Kit was left largely unaffected by the introduction of GATA1 siRNA on the PU.1-KD cell (Fig. 2B). In contrast, the combinatorial introduction of GATA1 and GATA2 siRNAs severely reduced the expression levels of both markers (Fig. 2B). These results suggest that GATA1 compensates for the reduction in GATA2 and that its effect is independent of PU.1. Consistent with the observation in BMMCs, the FcεRIα mRNA level was increased in the PU.1-KD cells (Fig. 2D) despite the cell surface expression of FcεRI being decreased. Both the FcεRIα and FcεRIβ mRNA levels were markedly downregulated in the GATA1/GATA2 double-KD and GATA1/GATA2/PU.1 triple-KD cells (Fig. 2D). Consistent with the observation in BMMCs, GATA2 mRNA levels were increased in the PU.1-KD cells (Fig. 2E). In contrast, the increase in the level of GATA1 mRNA in the PU.1-KD cells was small and not statistically significant (Fig. 2E). The PU.1 mRNA level was not affected by the KD of a single GATA factor but was significantly upregulated in the GATA1/GATA2 double-KD cells (Fig. 2E). Notably, despite the high level of PU.1, the FcεRIβ mRNA level was significantly reduced in the GATA1/GATA2 double-KD cells (Fig. 2D). These data indicate that PU.1 is not able to activate the *Ms4a2* gene expression in the absence of these GATA factors.

Genomic occupation of PU.1 and GATA2 showed partially overlapping but distinct profiles at the *Ms4a2* locus. To determine the *cis*-acting region required for

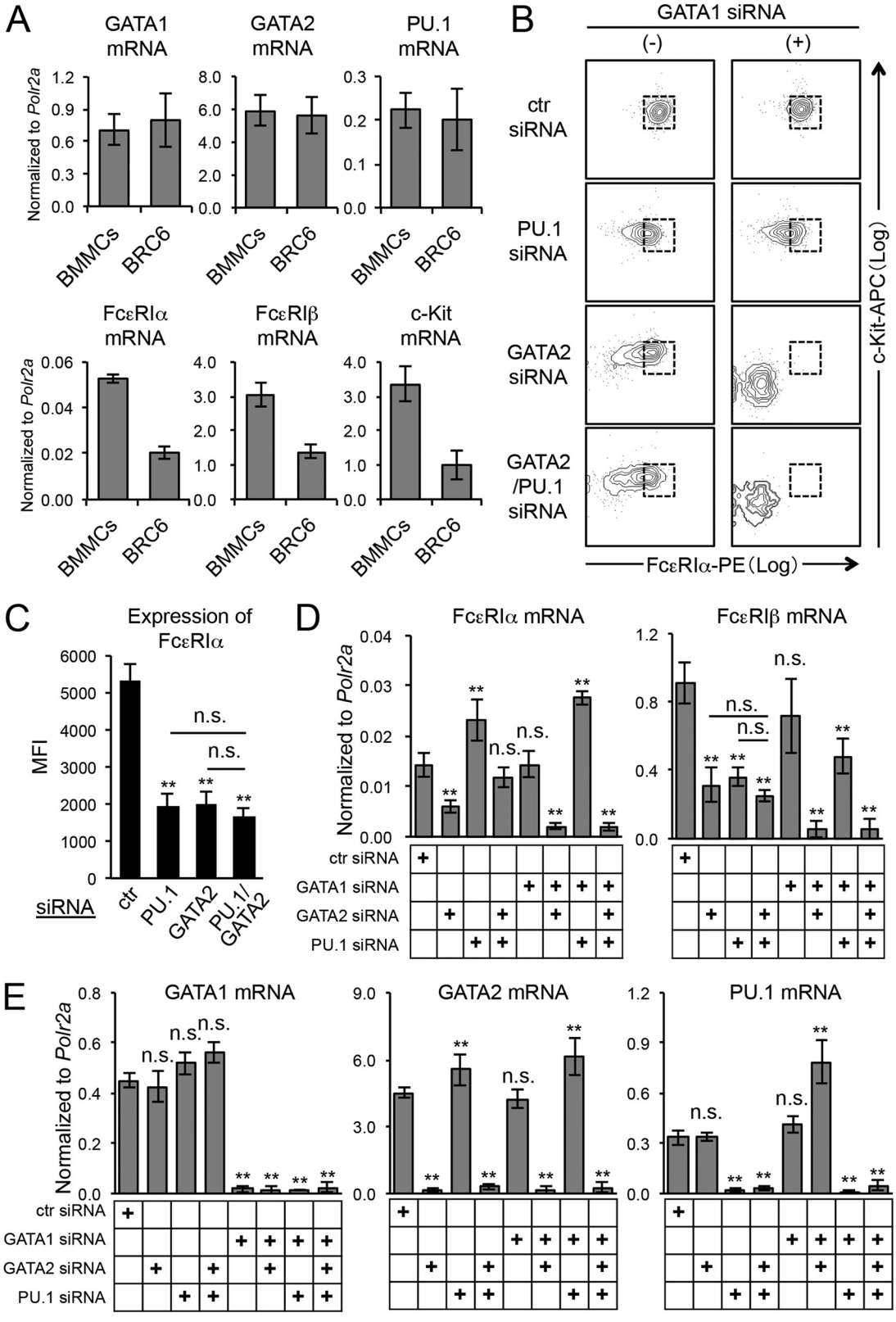

FIG 2 GATA1 and GATA2 coordinately regulate the expression of the *Ms4a2* gene. (A) Results of qRT-PCR analysis of the indicated genes in BMMCs and BRC6 cells. $n = 4$. (B) Representative FACS data for BRC6 cells cotransfected with the indicated siRNAs and pMAX enhanced GFP (eGFP) plasmid DNA. Data are representative of results from four independent experiments. ctr, control. (C) MFI of FcεRIα expression on BRC6 cells cotransfected with the indicated siRNAs and pMAX eGFP plasmid DNA. $n = 4$. (D and E) qRT-PCR of FcεRI subunits (FcεRIα and FcεRIβ) (D) and transcription factors (GATA1, GATA2, and PU.1) (E) in BRC6 cells cotransfected with the indicated siRNAs and pMAX eGFP plasmid DNA. The samples were prepared from the GFP-positive cell

(Continued on next page)

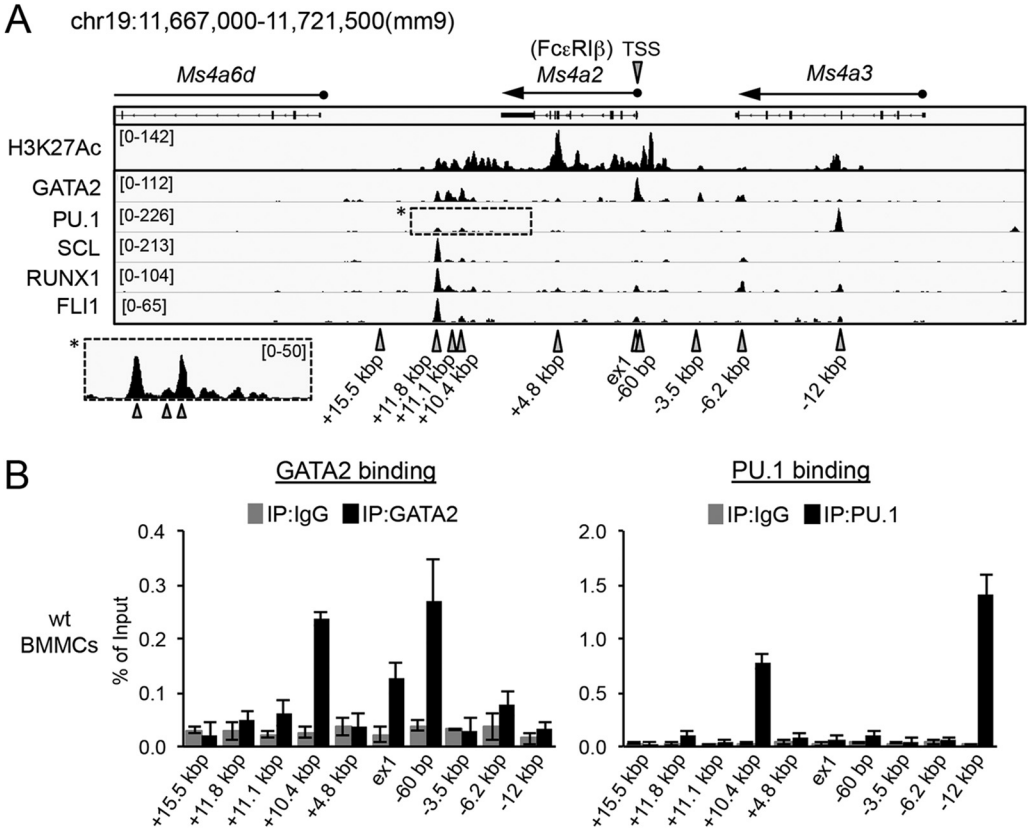

FIG 3 Genomic occupation of PU.1 and GATA2 showed partially overlapping but distinct profiles at the *Ms4a2* locus. (A) Publicly available ChIP-seq data of the histone modification marks and the binding of mast cell-related transcription factors at the *Ms4a2* locus in BMMCs (41). The peaks are visualized with IGV software. The numbers in the upper left of each track indicate track heights. The transcription start site (TSS) of the *Ms4a2* gene and the distance (in kilobase pairs) of each binding peak relative to the TSS are shown. Ex1 indicates exon1. The panel indicated with an asterisk presents an expanded view of the PU.1 binding at the +11.1-, +10.4-, and +10.2-kbp regions. The value was set to 50. (B) Binding of GATA2 and PU.1 to the *Ms4a2* locus was examined by quantitative ChIP (qChIP) assays. Chromatin fragments were prepared from wild-type (wt) BMMCs. The values of PCR amplicons determined using immunoprecipitated (IP) chromatin relative to those of the input samples are shown. The results were obtained from four independent assays. The +15.5-kbp region was amplified as a negative-control region for GATA2 and PU.1 binding.

Ms4a2 gene expression, we utilized publicly available ChIP sequencing (ChIP-seq) data from a previous study of BMMCs (41) for binding of several transcription factors, including GATA2 and PU.1, and for acetylation of H3K27 (H3K27ac), a marker of active enhancers and promoters (42, 43) (Fig. 3A). On the basis of these data, we prepared primers that amplify several genomic regions showing binding peaks of GATA2 or PU.1 and performed a ChIP-quantitative PCR (ChIP-qPCR) analysis in wild-type (wt) BMMCs (Fig. 3B). The +10.4-kbp and −60-bp regions were bound by GATA2, whereas the +11.8-kbp and +11.1-kbp peaks of the ChIP-seq data showed only weak binding by GATA2 in the ChIP-qPCR analysis. The PU.1 binding peaks were observed at the +10.4-kbp and −12-kbp regions. Although the intensity of the PU.1 binding was lower at the +10.4-kbp peak than at the −12-kbp peak, the peaks were clearly observed compared to those at the neighboring regions (Fig. 3A).

In order to determine whether or not the GATA2 and PU.1 binding profiles are specific to mast cells, ChIP-qPCR analysis was performed using BRC6, murine erythroleukemia (MEL), and murine myeloid 32Dcl3 cells (Fig. 4). The GATA2 mRNA and protein

FIG 2 Legend (Continued)
populations. For panels B and C, GFP-positive cells were analyzed. For panels C, D, and E, the data were analyzed by one-way ANOVA with Dunnett's *post hoc* test and compared to those from the ctr siRNA transfected cells and additionally compared as indicated. *, $P < 0.05$; **, $P < 0.01$; n.s., not significant.

levels were lower in MEL cells than in the other cell lines, whereas PU.1 was detectable in all cell lines examined (Fig. 4A to C). The absence of the FcεRIβ mRNA and protein expression in non-mast cell lines MEL and 32Dcl3 was confirmed (Fig. 4A to C). The ChIP-qPCR analysis revealed that the levels of GATA2 binding in BRC6 cells were similar to those in BMMCs (Fig. 3B; Fig. 4D). There was no detectable binding of GATA2 throughout the *Ms4a2* locus in MEL cells (Fig. 4D). In 32Dcl cells, GATA2 binding to the +10.4-kbp region was observed, whereas binding to exon 1 (ex1) and the −60-bp region was not detected. The PU.1 binding to the +10.4-kbp and −12-kbp regions was similarly observed in all cell lines, regardless of the level of *Ms4a2* gene expression (Fig. 4D). These data indicate that GATA2, but not PU.1, binds to the proximal −60-bp region specifically in mast cells.

PU.1 facilitates GATA2 binding to the +10.4-kbp and −60-bp regions and functions cooperatively with LDB1. On the basis of our ChIP-qPCR data, we considered that PU.1 might regulate the *Ms4a2* gene by facilitating GATA2 binding to the proximal −60-bp region. As predicted, ChIP-qPCR analysis of BMMCs from *Spi1*$^{f/f}$::*CreER*^{T2} mice revealed that the GATA2 binding to the −60-bp region decreased over time with 4-OHT treatment (Fig. 5A). Interestingly, the GATA2 binding to the +10.4-kbp region was even more sharply reduced by the PU.1 ablation on day 3 of 4-OHT treatment (Fig. 5A), concurrent with the reduction in the levels of FcεRIβ mRNA (Fig. 1C). These data suggest that the +10.4-kbp region, bound by both GATA2 and PU.1, plays a key role in *Ms4a2* gene expression.

Suspecting that this region might reside in close proximity to the proximal −60-bp region as a consequence of chromatin looping, we next investigated the contribution of LDB1. Since this factor has been shown to facilitate chromatin loop formation of the genes regulated by the GATA factors or PU.1 (27–30), we speculate that the +10.4-kbp and −60-bp regions were bound by LDB1. As expected, ChIP-qPCR analysis revealed that the +10.4-kbp and −60-bp regions were bound by LDB1 in BMMCs and that PU.1 ablation significantly reduced the binding activity (Fig. 5B). Furthermore, KD experiments showed that introduction of LDB1 siRNA into BRC6 cells significantly reduced the FcεRIβ mRNA level (Fig. 5C). Interestingly, simultaneous KD of LDB1 and PU.1 further decreased the FcεRIβ mRNA level (Fig. 5C). A FACS analysis showed that the introduction of LDB1 siRNA by itself reduced the FcεRI expression and that combinatorial reductions in LDB1 and GATA2 or PU.1 further reduced the mean fluorescent intensity (MFI) of FcεRI (Fig. 5D). These results suggest that PU.1 and LDB1 cooperatively regulate *Ms4a2* gene expression by binding to the +10.4-kbp region.

The deletion of the +10.4-kbp region completely abrogated expression of the *Ms4a2* gene in BRC6 mast cells. In order to determine the requirement of the +10.4-kbp region for the *Ms4a2* gene expression, we performed CRISR/Cas9-mediated targeted deletion of the +10.4-kbp region in BRC6 cells. A sequence examination revealed that this region contains 3 and 2 consensus binding sequences for PU.1 and GATA2, respectively (Fig. 6A). To delete the +10.4-kbp region, 4 single guide RNAs (sgRNAs) (sgRNA 1 to 4) were set at the +11.8/+10.2-kbp region (Fig. 6B). Following the introduction of the sgRNAs and selections, deletion of the target region was examined by quantitative PCR amplification of the +11.1-, +10.4-, and +10.2-kbp regions using genomic DNA (Fig. 6B and C). The data were normalized with the quantitative PCR amplification of the −60-bp region, which was not affected by the genome editing. It was revealed that 7 and 8 clones were heterozygous and homozygous deletion mutants, respectively. Among the homozygotes, three clones were obtained from the introduction of sgRNAs 1 and 4, four clones were obtained from the introduction sgRNAs 1 and 3, and one was obtained from the introduction of sgRNAs 2 and 3 (Fig. 6C).

We next examined the mRNA levels of PU.1, GATA2, and FcεRIβ by qRT-PCR analysis (Fig. 7A and B). Including the wt clones that did not show genomic deletion in the +11.8/+10.2-kbp region, the CRISPR/Cas9-mediated genome editing *per se* did not affect the PU.1 or GATA2 mRNA levels (Fig. 7A). Remarkably, the FcεRIβ mRNA was significantly reduced in level and undetectable in the heterozygous and homozygous

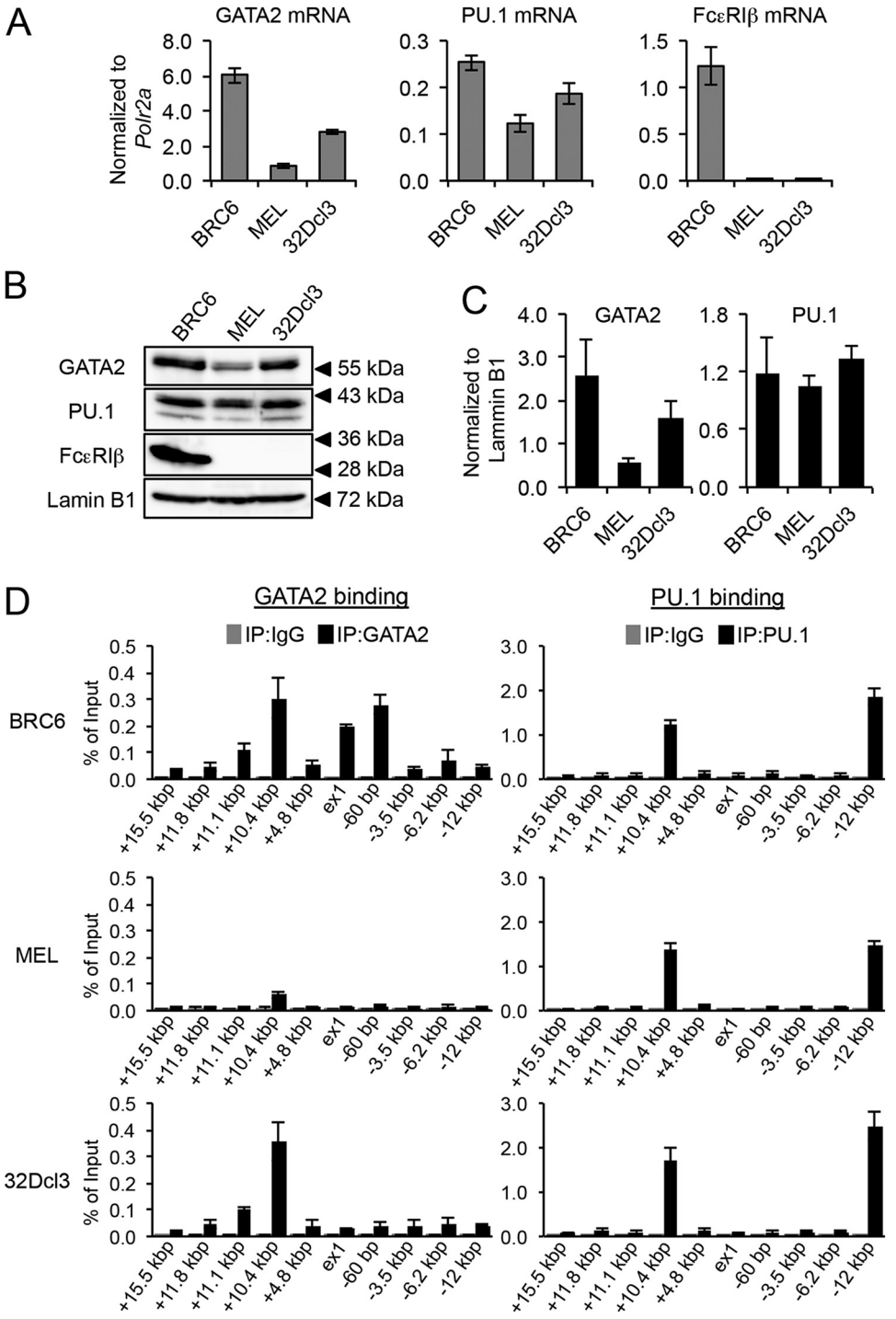

FIG 4 mRNA and protein expression of GATA2, PU.1, and FcεRIβ in non-mast cell lines MEL and 32Dcl3. (A) Results of qRT-PCR analyses of the indicated genes in BRC6 cells, MEL cells (a murine erythroleukemia cell line), and 32Dcl3 cells (a murine myeloid cell line). $n = 4$. (B) Expression of GATA2, PU.1, FcεRIβ, and lamin B1 (control) proteins was analyzed by Western blotting. The arrowheads indicate the positions of marker protein. (C) Densitometry analysis was performed on the GATA2 and PU.1 blots shown in panel B, and the intensities of the GATA2 and PU.1 bands relative to those of lamin B1 were measured using the Image J software program (NIH, USA). For panel B, the data are representative of results from four independent experiments. (D) Binding of GATA2 and PU.1 to the *Ms4a2* locus was examined by ChIP-qPCR assays. Chromatin fragments were prepared from BRC6, MEL, and 32Dcl3 cells. The values determined for PCR amplicons using immunoprecipitated chromatin relative to those of the input samples are shown. The results were obtained from four independent assays.

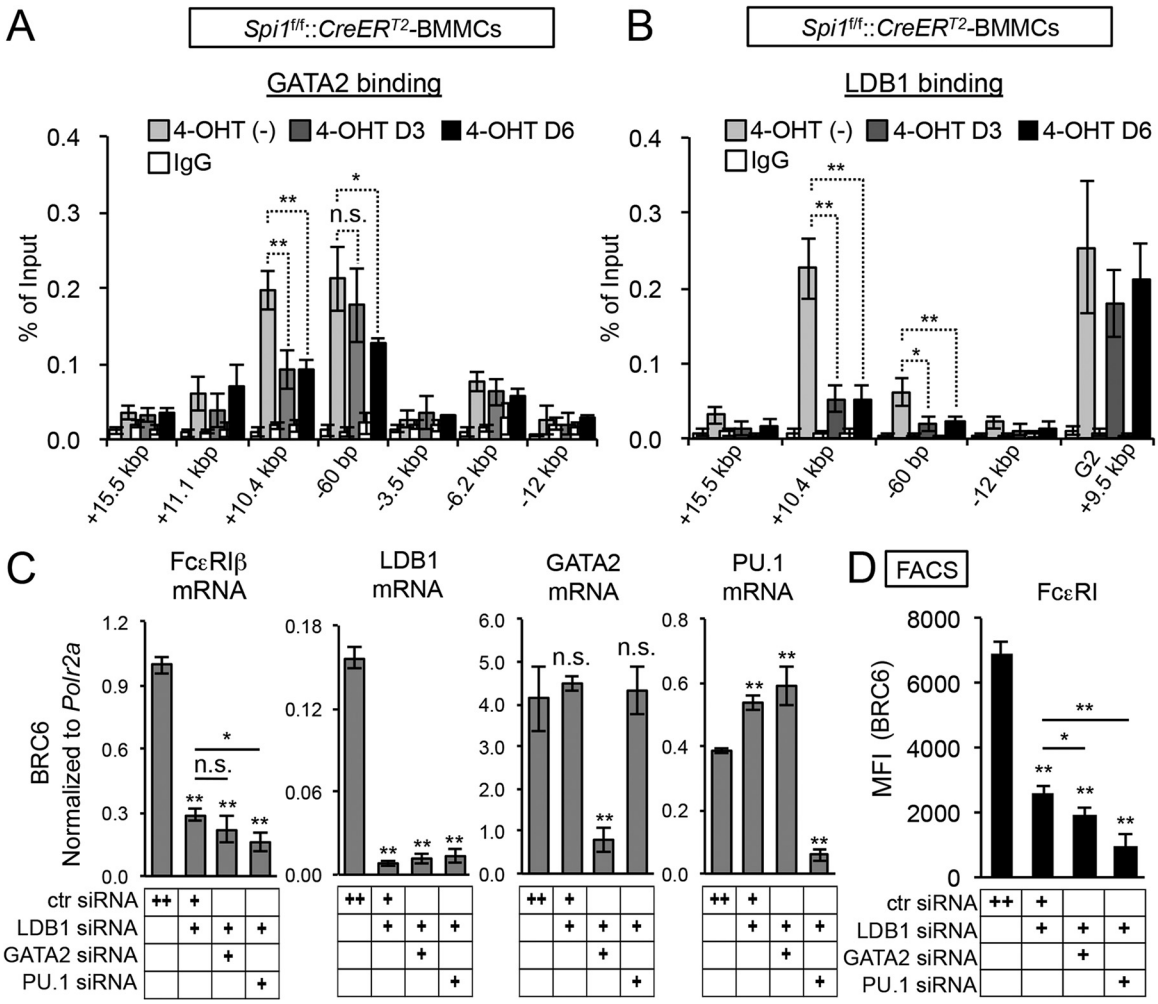

FIG 5 Conditional ablation of PU.1 in BMMCs resulted in a significant reduction in the level of GATA2 binding to the −60-bp region as well as in the levels of GATA2 and LDB1 binding to the +10.4-kbp region. (A and B) Genomic binding of GATA2 (A) and LDB1 (B) to the *Ms4a2* locus was examined by ChIP-qPCR assays. Chromatin fragments were prepared from *Spi1*$^{f/f}$::*CreER*^{T2} BMMCs after 0, 3, and 6 days of 4-OHT treatment. The values determined for the PCR amplicons using immunoprecipitated chromatin relative to those of the input sample are shown. The results were obtained from four independent assays. For panel B, *Gata2* (G2) +9.5 kbp was amplified as a positive-control region for LDB1 binding. (C) qRT-PCR of FcεRIβ, LDB1, GATA2, and PU.1 in BRC6 cells cotransfected with the indicated siRNAs. Cells were cotransfected with pMAX eGFP plasmid DNA, and the samples were prepared from GFP-positive cell populations. $n = 5$. (D) MFI of FcεRI expression in LDB1-KD cells. Samples were prepared from BRC6 cells cotransfected with the indicated siRNAs and pMAX eGFP plasmid DNA. The MFI of the GFP-positive cells is shown. $n = 5$. All data were analyzed by one-way ANOVA with Dunnett's *post hoc* test. For panels A and B, data were compared as indicated. For panels C and D, data were compared to those from the ctr siRNA transfected cells and were additionally compared as indicated. *, $P < 0.05$; **, $P < 0.01$; n.s., not significant.

clones, respectively (Fig. 7B), suggesting that the FcεRIβ mRNA level is dependent on the gene dosage of the +10.4-kbp region. Consistent with these results, a FACS analysis showed a significant reduction in the FcεRI expression level in the homozygous clones (Fig. 7C), and the MFI of FcεRIα was significantly reduced in the heterozygous clones (Fig. 7D). As observed in the PU.1 KO BMMCs (Fig. 5A), the ChIP-qPCR analysis revealed that deletion of the +10.4-kbp region significantly reduced the GATA2 binding activity with respect to the −60-bp region (Fig. 7E). Furthermore, the level of PU.1 binding to the −12-kbp region was significantly reduced by the deletion of the +10.4-kbp region (Fig. 7E). These results indicate that the +10.4-kbp region regulates the binding of GATA2 and PU.1 to the −60-bp and −12-kbp regions, respectively, and plays central roles in *Ms4a2* expression.

The −12-kbp region is required to achieve the maximum level of *Ms4a2* gene expression. To determine whether or not the −12-kbp region contributes to *Ms4a2* gene expression, this region was deleted by CRISR/Cas9-mediated genome editing (Fig.

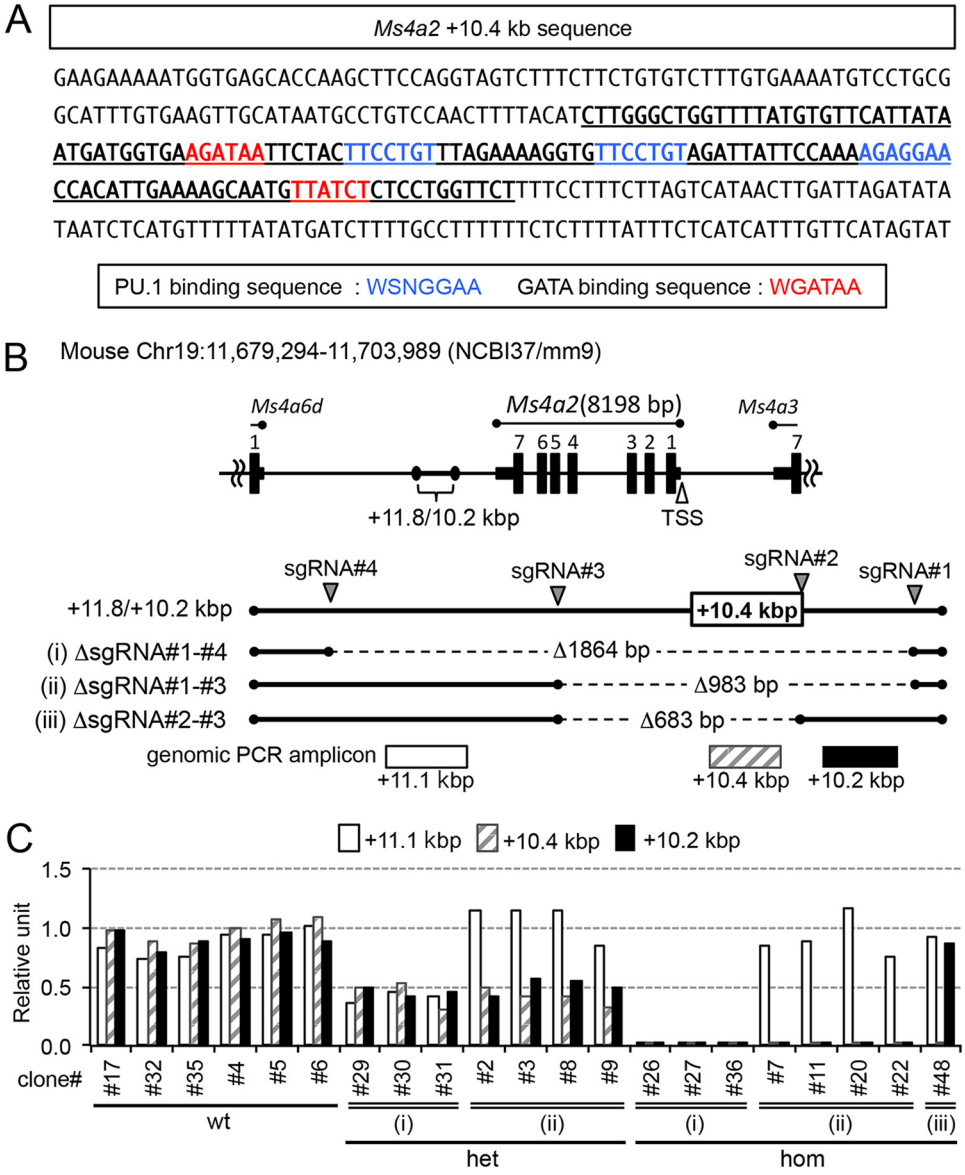

FIG 6 Scheme for targeted deletion of the +10.4-kbp region in BRC6 cells. (A) Nucleotide sequence of the +10.4-kbp region of the *Ms4a2* gene. The PCR fragments (+10.4 kbp) of the ChIP-qPCR are indicated in bold and underlined. Putative PU.1 and GATA2 binding sites are indicated in blue and red, respectively. (B) Schematic diagram of the *Ms4a2* gene with indicated positions of the +11.8/+10.2-kbp regions and the TSS. The positions of exons 1 to 7 and of the neighboring genes (*Ms4a6d* and *Ms4a3*) are also indicated. The schematic diagram shows the deleted regions of the CRISPR-Cas9 genome editing from the combination of guide RNAs (gRNAs) 1 and 4 (i), 1 and 3 (ii), and 2 and 3 (iii). Boxes indicate the positions of the PCR amplicons corresponding to +11.1, +10.4, and +10.2 kbp in panel C. (C) Determination of the genome-edited BRC6 cells by quantitative PCR. The +11.1-, +10.4-, and +10.2-kbp regions were amplified by quantitative PCR in the genome-edited BRC6 cells, and the values were normalized to that of the −60-bp region. The numbers indicate the clones. The estimated genotypes of wild-type, heterozygote, and homozygote are indicated as wt, het, and hom, respectively. The deletion mutant clones that resulted from the combinations of gRNAs 1 and 4, 1 and 3, and 2 and 3 are indicated as (i), (ii), and (iii), respectively.

8A). The average level of FcεRIβ mRNA was significantly lower in the homozygous clones lacking the −12-kbp region than in the wt clones, although the reduction was modest (Fig. 8B). There was a trend toward a lower MFI of FcεRI in the deletion mutants than in the wt clones, although the difference was not statistically significant in the FACS analysis (Fig. 8C). These results indicate that the −12-kbp region is required to achieve maximum *Ms4a2* gene expression, although its contribution is less than that of the +10.4-kbp region.

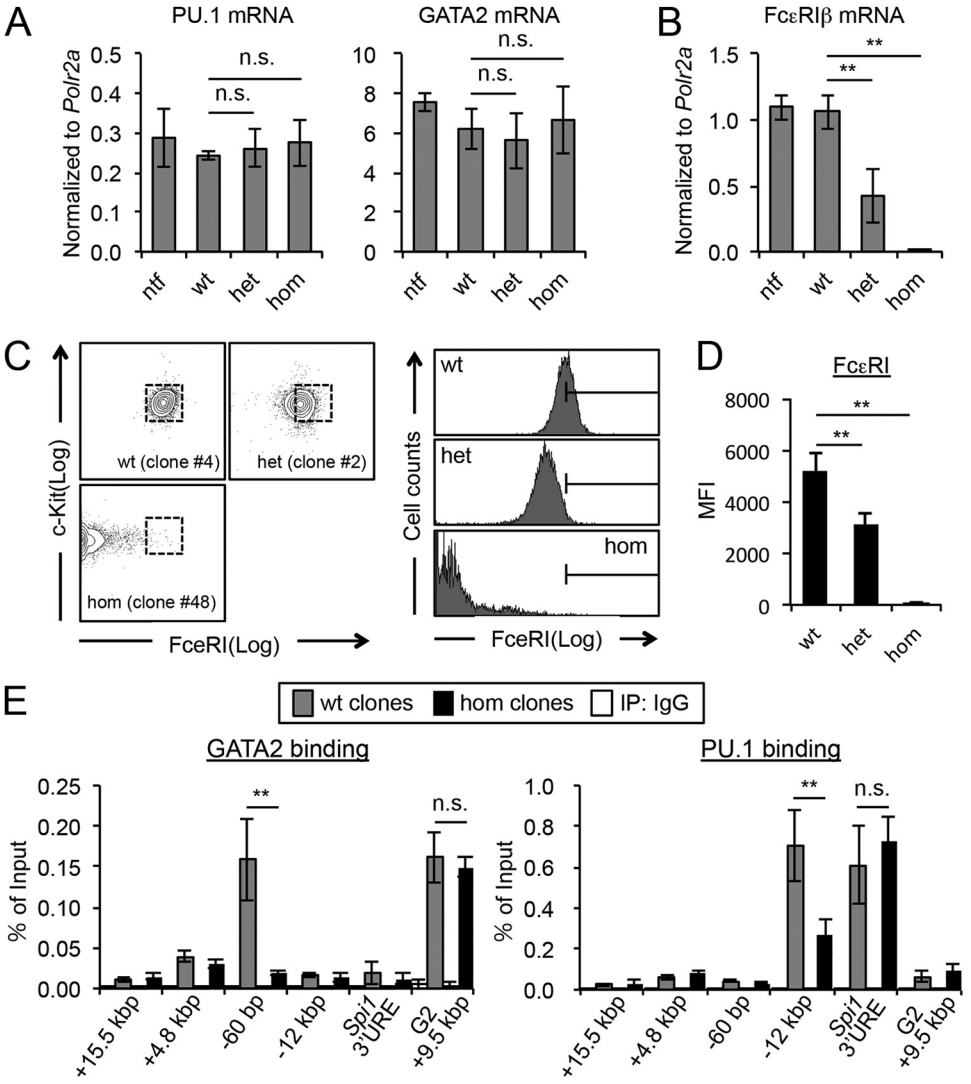

FIG 7 Deletion of the +10.4-kbp region completely abrogated *Ms4a2* gene expression in BRC6 mast cells. (A and B) Results of qRT-PCR of the indicated genes in genome-edited BRC6 cells. The samples were prepared from cells with no transfection (ntf, $n = 4$), cells without gene deletions (wt, $n = 6$), heterozygote cells (het, $n = 7$), and homozygote cells (hom, $n = 8$). (C and D) Representative FACS data (dot plot and histograms) (C) and the MFI (D) of the genome-edited BRC6 cells. For panel C, the samples were prepared from wt (clone 4), het (clone 2), and hom (clone 48) cells. (E) Genomic binding of GATA2 and PU.1 to the *Ms4a2* locus was examined by ChIP-qPCR assays. Chromatin fragments were prepared from wt and hom clones. The results were obtained from four independent assays. The values of PCR amplicons determined using immunoprecipitated chromatin relative to those of the input are shown. The *Spi1* 3′URE region and *Gata2* (G2) +9.5-kbp region were amplified as positive-control regions for PU.1 and GATA2 binding, respectively. For panels A, B, and D, the data were analyzed by one-way ANOVA with Dunnett's *post hoc* test and compared to the wt data. For panel E, data were compared as indicated. **, $P < 0.01$; n.s., not significant.

DISCUSSION

The present study showed that GATA2 and PU.1 cooperatively regulate *Ms4a2* gene expression through distinct mechanisms. We identified the distal *cis*-regulatory region that is indispensable for *Ms4a2* gene expression using CRISPR-Cas9-mediated genome editing. The schematic illustrations shown in Fig. 9 represent a summary of the results (Fig. 9A) and a predicted model (Fig. 9B).

Our data revealed the unique role of PU.1 in promoting the DNA binding activity of GATA2 and LDB1 at the *Ms4a2* locus. Furthermore, LDB1 appeared to be a novel positive regulator of *Ms4a2* gene expression according to KD studies. Interestingly, a recent study reported that PU.1 plays an essential role in the formation of the chromosome

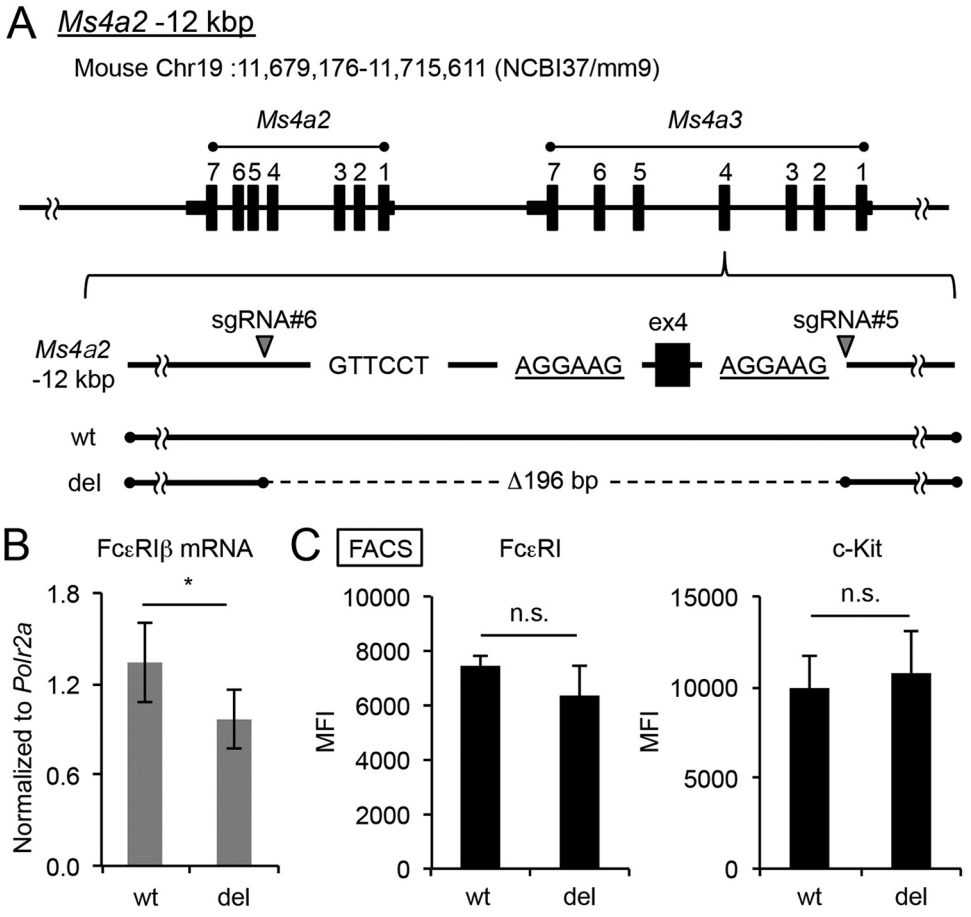

FIG 8 Deletion of the *Ms4a2* −12-kbp region affected the FcεRIα mRNA level moderately. (A) Schematic diagram of the *Ms4a2* and *Ms4a3* genes. The *Ms4a2* −12-kbp region is located upstream and downstream of the fourth exon. The arrowheads indicate the positions of sgRNAs 5 and 6 used in CRISPR-Cas9 genome editing. The putative PU.1 binding sites conserved between human and mouse are underlined. wt, wild type; del, deletion. (B) Results of qRT-PCR analysis of FcεRIβ mRNA expression in wild-type and *Ms4a2* −12-kbp-region-deleted BRC6 cells. The samples were prepared from undeleted (wt, $n = 5$) and homozygote (del, $n = 7$) cells. (C) MFI of FcεRI and c-Kit expression by the genome-edited BRC6 cells examined as described for panel B. For panels B and C, *, $P < 0.05$; n.s., not significant. Data were compared to the results determined for the wt.

architecture during *SPI1* gene autoregulation by recruiting LDB1 in human monocytes (30). Recent Hi-C experiments revealed that eukaryote chromatin is organized into compartments composed of topologically associating domains (TADs) that are critical chromosome structural domains in the regulation of long-range gene expression (47–49). TADs are further divided into smaller chromosomal units, termed SubTADs (50), that are characterized by enhanced intrachromosomal interactions. The study showed that PU.1 is required for the initial formation of a subTAD containing the *SPI1* gene and that, once these intrachromosomal interactions are established, LDB1 can maintain the structure in the absence of PU.1. Our data representing murine *Ms4a2* gene regulation showed that conditional ablation of PU.1 resulted in a significant reduction in the level of GATA2 binding to the −60-bp region as well as of GATA2 and LDB1 binding to the +10.4-kbp region, suggesting the persistent requirement of this factor for the maintenance of active chromatin architecture at the *Ms4a2* locus. Thus, the molecular basis of the PU.1-mediated chromatin structure formation of the *Ms4a2* locus likely overlaps to some degree, but is not identical to, that of *SPI1* autoregulation in human monocytes. To determine the chromosome architecture of the *Ms4a2* locus, chromosome conformation capture (3C) assays and related experiments need to be performed.

The CRISPR/Cas9 system is a powerful tool for assessing the impact of endogenous

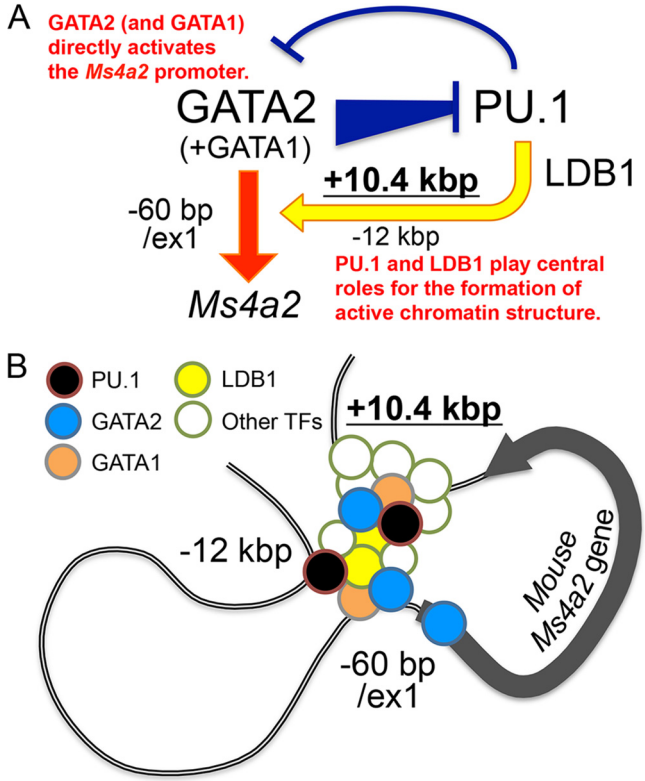

FIG 9 Schematic representation of the results. (A) Summary of the results. (B) A chromatin looping model for the regulation of the *Ms4a2* gene in mast cells.

enhancers on gene expression (51). The present study showed that deletion of the +10.4-kbp region almost completely eliminated *Ms4a2* gene expression in BRC6 cells. The impact of deletion on the FcεRIβ mRNA level was greater than that of the −12-kbp region bound by PU.1 as well as that of the ablation of transcription factors. The ChIP-seq analysis revealed that the +10.4-kbp region is bound by other transcription factors, such as SCL, RUNX1, and FLI1 (Fig. 3A). These factors might also contribute to *Ms4a2* gene expression. In addition, this region may be transcribed and may produce noncoding RNA, which might play a role in *Ms4a2* gene regulation. Recent mounting evidence suggests that transcripts from enhancer regions, designated enhancer RNAs (eRNAs), affect the enhancer function by facilitating local enhancer-promoter looping formation (52). In this regard, it would be interesting to determine whether or not the +10.4-kbp region is transcribed in mast cells.

The GATA factors, especially GATA1, and PU.1 have long been recognized as transcription factors that are "antagonistic" during hematopoietic development (9–15). During hematopoietic lineage decisions in multipotent hematopoietic stem and progenitor cells (HSPCs), GATA1 and PU.1 are coexpressed at low levels (53). Therefore, cross-inhibition of GATA1 and PU.1 has been considered a key molecular event during the lineage decision with regard to erythromegakaryocytic versus myeloid cells (54, 55). However, a recent study that tracked GATA1 and PU.1 protein expression at the single-cell level showed that expression of these factors rarely overlapped in HSPCs (56). Furthermore, a recent study using a computational method showed that both GATA1 and PU.1 become activated after the cell fate decision during the early phase of hematopoietic development (57). Interestingly, even though the GATA factors and PU.1 are coexpressed, we showed that the cross-inhibition of their respective expression levels was retained in mast cells. Cross-inhibition between the GATA factors and PU.1 might influence the expression of genes that are regulated by either factor individually. Indeed, we demonstrated that FcεRIα mRNA expression was dependent on the GATA

factors and was increased by reducing the level of PU.1 expression. Importantly, however, in the case of genes that are regulated by both factors, such as the *Ms4a2* gene, the gene expression can be regulated beyond the influence of the cross-inhibition and is dependent on how these factors act on the gene regulation. Thus, mast cell-specific genes can be classified into four groups, namely, the GATA factor-dependent, PU.1-dependent, coregulated, and unregulated gene groups. In the future, genome-wide gene expression analysis should be conducted to determine the classification of certain genes.

Only a few studies of *MS4A2* gene regulation in human mast cells have been performed. Consistent with our results in mouse BMMCs, it has been reported that GATA2 binds to the promoter region of the *MS4A2* gene in human mast cell line LAD2 (22). A comparison of the genomic sequences in mice and humans revealed that the consensus sequence for the PU.1 binding at the −12-kbp regions is also conserved between mice and humans. However, where the gene cassette composed of the mouse *Ms4a2* gene and the 3′-neighboring *Ms4a3* and *Oosp2* genes is located in the complementary strand, their human orthologues are positioned in the order *OOSP2*, *MS4A3*, and *MS4A2* in the forward direction. Furthermore, the distance between the human *MS4A2* gene and the 3′-neighboring *MS4A6A* gene (mouse orthologue of *Ms4a6d*) was approximately 73.1 kbp, which is much greater than that between the mouse *Ms4a2* gene and the 5′-neighboring *Ms4a6d* gene (approximately 10.7 kbp). These observations suggest that genomic loci containing the *Ms4a2*/*MS4A2* gene were dynamically reorganized during mammalian evolution. As anticipated, we were unable to find a candidate for a counterpart of the +10.4-kbp region of the mouse *Ms4a2* gene at the human *MS4A2* locus.

In addition to these differences, previous studies showed a negative regulatory region of human *MS4A2* gene that resides in the fourth intron of its own gene (58). This region is bound by a myeloid zinc finger protein 1 (MZF-1) and a repressor complex composed of FHL3, NFY, and HDAC1/2 (58, 59). Notably, the recognition sequence for MZF-1 is not conserved in the mouse *Ms4a2* gene. Taken together, these data suggest that the molecular basis underlying the *Ms4a2*/*MS4A2* gene regulation is not conserved between mice and humans at several points.

In summary, we demonstrated that GATA2 and PU.1 regulate *Ms4a2* gene expression through distinct molecular mechanisms. Although the binding of GATA2 and PU.1 to the +10.4-kbp region is not mast cell specific, this region is indispensable for the *Ms4a2* gene expression and likely plays a central role in forming an active chromatin structure in murine mast cells.

MATERIALS AND METHODS

Mice. *Spi1*$^{flox/flox}$ mice (60) were purchased from Jackson Laboratories (stock no. 006922). *Gata2*$^{flox/flox}$ mice (61) were kindly provided by S. A. Camper (University of Michigan, MI). The z4-hydroxytamoxifen (4-OHT)-inducible *Rosa26CreER*^{T2} mice were kindly provided by Anton Berns (Netherlands Cancer Institute, Amsterdam, The Netherlands). The *Spi1* or *Gata2* knockout phenotype was examined in BMMCs prepared from homozygous male mice expressing CreER^{T2}. In both mutant mice, the genomic region encoding the DNA binding domain was deleted as a result of Cre-loxP-mediated recombination. The mice were maintained in an animal facility of Takasaki University of Health and Welfare in accordance with institutional guidelines.

Cell culture. Bone marrow cells were harvested from the femurs of 8- to 12-week-old mice and cultured with RPMI 1640 medium (Nacalai Tesque) supplemented with 10% fetal bovine serum (FBS; Gibco), 1% streptomycin-penicillin (Nacalai Tesque), 10 ng/ml recombinant murine interleukin-3 (IL-3; Peprotech) and 10 ng/ml recombinant murine (Peprotech). BMMCs were generated as described previously (44). On cell culture day 30, when almost all (>95%) of the cells were positive for c-Kit and FcεRIα as determined by fluorescence-activated cell sorter (FACS) analysis, the BMMCs were treated with 0.5 μM 4-OHT to induce Cre-mediated recombination. MEDMC-BRC6 cells (40) were purchased from RIKEN BRC (Tsukuba, Japan) and cultured in Iscove's modified Dulbecco's medium (IMDM; Invitrogen) containing the following: 15% fetal bovine serum (FBS), ITS liquid medium supplement (Sigma), 50 mg/ml ascorbic acid (Sigma), 0.45 mM α-monothioglycerol (Sigma), 3 ng/ml IL-3, 30 ng/ml stem cell factor (SCF), 1% penicillin-streptomycin solution, and 2 mM L-glutamine (Nacalai Tesque). Murine erythroleukemia (MEL) cells and 32Dcl3 cells (murine myeloid progenitor cell line) were cultured as previously described (44).

Western blotting. Cytoplasmic extracts were prepared as previously described (45). Cytoplasmic proteins were resolved by 10% SDS-polyacrylamide gel electrophoresis, and Western blot analysis was performed as previously described using anti-lamin B1 (ab16048; Abcam), anti-α-tubulin (T9026; Sigma-

TABLE 1 Primer sequences for ChIP-qPCR analyses

Primer	Sequence (5′ to 3′)	
	Forward	Reverse
Ms4a2		
+15.5 kbp	ACAGTGCAGAGGAGACGAGT	CCAGGCTTTCAGTGCCAGAT
+11.8 kbp	ACTGATGCGACCAGCTTCAT	GTCGGGGCTATGCTCTTCAG
+11.1 kbp	AAGCTTCTGAGGTGCTGAAC	GCTGAGACTTGCTTAGGTGATG
+10.8 kbp	ACACTGGCTGGACAATAAGC	GCAGGCAGACTTGATTTCAGC
+10.4 kbp	CTTGGGCTGGTTTTATGTGTTC	AGAACCAGGAGAGATAACATTGC
+10.2 kbp	AAGACTACCTGGAAGCTTGGTG	GGAAGGAAACAGATGCTTGTCC
+4.8 kbp	GCTGCTTTGTGGCTTCTTTC	GGAAGAGGAAGGGTTTTCACAC
ex1	TGTGGATTTGGGAGAGCAAGA	ATCCAGAGCACACCGCATTT
−60 bp	ACTGATATCAATCAGCCTGGAGAC	GGCAGTTAAGATGGGTTGACTC
−3.5 kbp	TGAGGGCCTGTGTTCAAATC	ATGTGTGCATGTGTGGACTC
−6.2 kbp	TTCCATTTCTGTGGGTTGCC	ATAGGGGCAAGCAGAAACAC
−12 kbp	ACCCACCCTCTGTTTTCTACTG	ACACGAATGCTGGTAAGTGC
Gata2, +9.5 kbp	ACATCTGCAGCCGGTAGATAAG	CATTATTTGCAGAGTGGAGGGTATTA
Spi1, 3′URE	CTGGTGGCAAGAGCGTTTC	ACGCCAACAGCCCCATTAC

Aldrich), anti-GATA2 (B9922A; Perseus Proteomics), anti-PU.1 (C-3; Santa Cruz), anti-FcεRIβ (H-5; Santa Cruz), and anti-FcεRIα (MAR-1; Invitrogen). The signal was visualized using Immobilon Western chemiluminescent horseradish peroxidase (HRP) substrate (Merck).

Chromatin immunoprecipitation (ChIP) assay. The ChIP assay and quantitative analysis of DNA purified from the ChIP samples were conducted as described previously (44). The antibodies used for ChIP assay were anti-PU.1 (C-3; Santa Cruz), anti-GATA2 (B9922A; Perseus Proteomics), anti-LDB1 (N2C3; GeneTex), normal rabbit IgG (2729S; Cell Signaling Technology) and normal mouse IgG2b (E7Q5L; Cell Signaling Technology). The DNA purified from ChIP samples was analyzed using an Mx3000P real-time PCR system (Agilent) with GoTaq qPCR master mix (Promega). The primers used for the ChIP assays are shown in Table 1.

siRNAs and transfection. The small interfering RNA (siRNA) duplexes for mouse GATA1 (assay identifiers [ID] RSS303126, RSS303127, and RSS303128), GATA2 (assay ID MSS204584, MSS204585, and MSS274487), PU.1 (assay ID MSS247676, MSS247678, and MSS277025), and LDB1 (assay ID MSS205922, MSS205923, and MSS205924) were purchased from Thermo Scientific. Control siRNA (SIC-001) was purchased from Sigma. MEDMC-BRC6 cells (2.0×10^6) or BMMCs (2.5×10^6) were cotransfected with 1.0 μg of green fluorescent protein (GFP)-encoding plasmid and a pool of two or three different siRNAs (10 nM each) by electroporation using NEPA21 (Nepa Gene Co., Tokyo, Japan). At 24 h after transfection, cells were sorted to obtain the GFP-expressing cells using a FACSJazz cell sorter (BD Biosciences).

Reverse transcription-PCR (RT-PCR). Isolation of total RNA was performed using NucleoSpin RNA (Macherey-Nagel). The reverse transcription reactions were performed using a ReverTra Ace qPCR RT kit (Toyobo) according to the manufacturer's instructions. Synthesized cDNAs were analyzed using an Mx3000P real-time PCR system (Agilent) with GoTaq qPCR master mix (Promega) as previously described (44). The results were normalized to polymerase (RNA) II (DNA-directed) polypeptide A gene (*Polr2a*). The primers used for quantitative reverse transcription-PCR (qRT-PCR) are shown in Table 2.

Fluorescence-activated cell sorter (FACS) analysis. The cells were stained with allophycocyanin (APC)-conjugated rat anti-mouse CD117 (c-Kit [clone 2B8]; BD Pharmingen) and phycoerythrin (PE)-conjugated mouse anti-mouse FcεRIα (clone MAR-1; eBioscience). Flow cytometric analyses were performed using a FACSCanto II flow cytometer (BD Biosciences).

CRISPR/Cas9 genome editing. CRISPR/Cas9-mediated genomic editing was performed using pSpCas9(BB)-2A-Puro (PX459) V2.0 and pSpCas9(BB)-2A-GFP (PX458). These plasmid DNAs (Addgene plasmid 48138 and 48139) were a gift from Feng Zhang (46). Single-guide RNAs (sgRNAs) targeting the

TABLE 2 Primer sequences for qRT-PCR analyses

Primer for qRT-PCR	Sequence (5′ to 3′)	
	Forward	Reverse
Polr2a	CTGGACCCTCAAGCCCATACAT	CGTGGCTCATAGGCTGGTGAT
Spi1	AGAAGCTGATGGCTTGGAGC	GCGAATCTTTTTCTTGCTGCC
Gata1	CAGAACCGGCCTCTCATCC	TAGTGCATTGGGTGCCTGC
Gata2	GCACCTGTTGTGCAAATTGT	GCCCCTTTCTTGCTCTTCTT
Ldb1	CACGCTACTTCCGAAGCATTT	TGCTGAAGTGCCACGTCTTT
Fcer1a	AGAGCAAACCTGTGTACTTG	GTGGACTTTCCATTTCTTCC
Ms4a2	AGGCTATCCATTCTGGGGTG	GGCTGCCTCTCACCAGATAC
Kit	AGCAATGGCCTCACGAGTTCTA	CCAGGAAAAGTTTGGCAGGAT

TABLE 3 Sequences of gRNAs complementary to target sites

sgRNA	Target sequence (5′ to 3′)
Ms4a2 (+11.8/10.2-kbp)	
1	TGGAATGAGAAAGGTTCATCTGG
2	CCTGCGGCATTTGTGAAGTTGCA
3	TCAGGCTTCTCAGCGGCTGTGGG
4	CCACGGATTGTCAATAGAACCCG
Ms4a2 (−12-kbp)	
5	CCTGTGCATTAAACGAGACTTGG
6	ATAGGAAGTAGGACGGATAAAGG

+11.8/10.2-kbp and −12-kbp regions of the *Ms4a2* gene were designed using CRISPRdirect (https://crispr.dbcls.jp). The target sequences are shown in Table 3. BRC6 cells were cotransfected with pX459 and pX458 vectors harboring a target sequence to express sgRNAs and Cas9 protein by electroporation using NEPA21 (Nepa Gene Co.). At 24 h after electroporation, the cells were cultured with 1.5 μg/ml of puromycin, and the GFP-positive cells were sorted using a FACSJazz cell sorter into 96-well plates. The genomic deletion was examined by quantitative PCR using genomic DNA isolated with PBND buffer (10 mM Tris-HCl [pH 8.3], 50 mM KCl, 0.1 mM $MgCl_2$, 0.1 mg/ml gelatin, 0.45% NP-40, 0.45% Tween 20, 200 μg/ml proteinase K). For homozygous deletion mutants, deletion of the entire +10.4-kbp region was further confirmed by DNA sequencing.

ChIP-seq data processing. The previously described ChIP-seq data sets (GSE48085) (41) were aligned to the mouse genome (mm9 assembly). The data (for GATA2, GSM1167578; for PU.1, GSM1167581; for SCL, GSM1167583; for RUNX1, GSM1167582; for Fli1, GSM1167577; for H3K27Ac, GSM1329816) were visualized using the Integrative Genomics Viewer (IGV).

Statistical analyses. The data are presented as means ± standard deviations (SD). Unless otherwise specified, comparisons between two groups were performed using an unpaired Student *t* test. Comparisons among multiple groups were performed using one-way analysis of variance (ANOVA) with Dunnett's test or Tukey's *post hoc* test and KaleidaGraph version 4.5 (Hulinks Inc.). For all analyses, statistical significance was defined as a *P* value of <0.05.

ACKNOWLEDGMENTS

We thank Taro Takeuchi for technical assistance.

This work was supported by a Grant-in-Aid for Scientific Research (C) from the Japan Society for the Promotion of Science (grants 18K06920 to K.O. and 17K08643 to S.O.).

Our contributions were as follows: conceptualization, S.O. and K.O.; methodology, S.O. and K.O.; investigation, S.O., Y.I., S.N., M.T., M.S., T.S., and K.C.; writing—original draft, S.O. and K.O.; writing—review and editing, K.O.; funding acquisition, S.O. and K.O.; resources, S.O., M.Y., and K.O.; supervision, K.O.

We declare that we have no competing financial interests.

REFERENCES

1. Pevny L, Lin CS, D'Agati V, Simon MC, Orkin SH, Costantini F. 1995. Development of hematopoietic cells lacking transcription factor GATA-1. Development 121:163–172.
2. Fujiwara Y, Browne CP, Cunniff K, Goff SC, Orkin SH. 1996. Arrested development of embryonic red cell precursors in mouse embryos lacking transcription factor GATA-1. Proc Natl Acad Sci U S A 93:12355–12358. https://doi.org/10.1073/pnas.93.22.12355.
3. Takahashi S, Onodera K, Motohashi H, Suwabe N, Hayashi N, Yanai N, Nabesima Y, Yamamoto M. 1997. Arrest in primitive erythroid cell development caused by promoter-specific disruption of the GATA-1 gene. J Biol Chem 272:12611–12615. https://doi.org/10.1074/jbc.272.19.12611.
4. Gutierrez L, Tsukamoto S, Suzuki M, Yamamoto-Mukai H, Yamamoto M, Philipsen S, Ohneda K. 2008. Ablation of Gata1 in adult mice results in aplastic crisis, revealing its essential role in steady-state and stress erythropoiesis. Blood 111:4375–4385. https://doi.org/10.1182/blood-2007-09-115121.
5. Tsai FY, Keller G, Kuo FC, Weiss M, Chen J, Rosenblatt M, Alt FW, Orkin SH. 1994. An early haematopoietic defect in mice lacking the transcription factor GATA-2. Nature 371:221–226. https://doi.org/10.1038/371221a0.
6. Tsai FY, Orkin SH. 1997. Transcription factor GATA-2 is required for proliferation/survival of early hematopoietic cells and mast cell formation, but not for erythroid and myeloid terminal differentiation. Blood 89:3636–3643.
7. Scott EW, Simon MC, Anastasi J, Singh H. 1994. Requirement of transcription factor PU.1 in the development of multiple hematopoietic lineages. Science 265:1573–1577. https://doi.org/10.1126/science.8079170.
8. McKercher SR, Torbett BE, Anderson KL, Henkel GW, Vestal DJ, Baribault H, Klemsz M, Feeney AJ, Wu GE, Paige CJ, Maki RA. 1996. Targeted disruption of the PU.1 gene results in multiple hematopoietic abnormalities. EMBO J 15:5647–5658. https://doi.org/10.1002/j.1460-2075.1996.tb00949.x.
9. Nerlov C, Graf T. 1998. PU.1 induces myeloid lineage commitment in multipotent hematopoietic progenitors. Genes Dev 12:2403–2412. https://doi.org/10.1101/gad.12.15.2403.
10. Rekhtman N, Radparvar F, Evans T, Skoultchi AI. 1999. Direct interaction of hematopoietic transcription factors PU.1 and GATA-1: functional antagonism in erythroid cells. Genes Dev 13:1398–1411. https://doi.org/10.1101/gad.13.11.1398.
11. Zhang P, Behre G, Pan J, Iwama A, Wara-Aswapati N, Radomska HS, Auron PE, Tenen DG, Sun Z. 1999. Negative cross-talk between hematopoietic regulators: GATA proteins repress PU.1. Proc Natl Acad Sci U S A 96:8705–8710. https://doi.org/10.1073/pnas.96.15.8705.

12. Nerlov C, Querfurth E, Kulessa H, Graf T. 2000. GATA-1 interacts with the myeloid PU.1 transcription factor and represses PU.1-dependent transcription. Blood 95:2543–2551.
13. Zhang P, Zhang X, Iwama A, Yu C, Smith KA, Mueller BU, Narravula S, Torbett BE, Orkin SH, Tenen DG. 2000. PU.1 inhibits GATA-1 function and erythroid differentiation by blocking GATA-1 DNA binding. Blood 96:2641–2648.
14. Arinobu Y, Mizuno S, Chong Y, Shigematsu H, Iino T, Iwasaki H, Graf T, Mayfield R, Chan S, Kastner P, Akashi K. 2007. Reciprocal activation of GATA-1 and PU.1 marks initial specification of hematopoietic stem cells into myeloerythroid and myelolymphoid lineages. Cell Stem Cell 1:416–427. https://doi.org/10.1016/j.stem.2007.07.004.
15. Burda P, Vargova J, Curik N, Salek C, Papadopoulos GL, Strouboulis J, Stopka T. 2016. GATA-1 inhibits PU.1 gene via DNA and histone H3K9 methylation of its distal enhancer in erythroleukemia. PLoS One 11:e0152234. https://doi.org/10.1371/journal.pone.0152234.
16. Du J, Stankiewicz MJ, Liu Y, Xi Q, Schmitz JE, Lekstrom-Himes JA, Ackerman SJ. 2002. Novel combinatorial interactions of GATA-1, PU.1, and C/EBPepsilon isoforms regulate transcription of the gene encoding eosinophil granule major basic protein. J Biol Chem 277:43481–43494. https://doi.org/10.1074/jbc.M204777200.
17. Baba Y, Maeda K, Yashiro T, Inage E, Niyonsaba F, Hara M, Suzuki R, Ohtsuka Y, Shimizu T, Ogawa H, Okumura K, Nishiyama C. 2012. Involvement of PU.1 in mast cell/basophil-specific function of the human IL1RL1/ST2 promoter. Allergol Int 61:461–467. https://doi.org/10.2332/allergolint.12-OA-0424.
18. Ohneda K, Moriguchi T, Ohmori S, Ishijima Y, Satoh H, Philipsen S, Yamamoto M. 2014. Transcription factor GATA1 is dispensable for mast cell differentiation in adult mice. Mol Cell Biol 34:1812–1826. https://doi.org/10.1128/MCB.01524-13.
19. Ohmori S, Moriguchi T, Noguchi Y, Ikeda M, Kobayashi K, Tomaru N, Ishijima Y, Ohneda O, Yamamoto M, Ohneda K. 2015. GATA2 is critical for the maintenance of cellular identity in differentiated mast cells derived from mouse bone marrow. Blood 125:3306–3315. https://doi.org/10.1182/blood-2014-11-612465.
20. Maeda K, Nishiyama C, Tokura T, Akizawa Y, Nishiyama M, Ogawa H, Okumura K, Ra C. 2003. Regulation of cell type-specific mouse Fc epsilon RI beta-chain gene expression by GATA-1 via four GATA motifs in the promoter. J Immunol 170:334–340. https://doi.org/10.4049/jimmunol.170.1.334.
21. Nishiyama C, Ito T, Nishiyama M, Masaki S, Maeda K, Nakano N, Ng W, Fukuyama K, Yamamoto M, Okumura K, Ogawa H. 2005. GATA-1 is required for expression of Fc{epsilon}RI on mast cells: analysis of mast cells derived from GATA-1 knockdown mouse bone marrow. Int Immunol 17:847–856. https://doi.org/10.1093/intimm/dxh278.
22. Inage E, Kasakura K, Yashiro T, Suzuki R, Baba Y, Nakano N, Hara M, Tanabe A, Oboki K, Matsumoto K, Saito H, Niyonsaba F, Ohtsuka Y, Ogawa H, Okumura K, Shimizu T, Nishiyama C. 2014. Critical roles for PU.1, GATA1, and GATA2 in the expression of human FcepsilonRI on mast cells: PU.1 and GATA1 transactivate FCER1A, and GATA2 transactivates FCER1A and MS4A2. J Immunol 192:3936–3946. https://doi.org/10.4049/jimmunol.1302366.
23. Oda Y, Kasakura K, Fujigaki I, Kageyama A, Okumura K, Ogawa H, Yashiro T, Nishiyama C. 2018. The effect of PU.1 knockdown on gene expression and function of mast cells. Sci Rep 8:2005. https://doi.org/10.1038/s41598-018-19378-y.
24. Agulnick AD, Taira M, Breen JJ, Tanaka T, Dawid IB, Westphal H. 1996. Interactions of the LIM-domain-binding factor Ldb1 with LIM homeodomain proteins. Nature 384:270–272. https://doi.org/10.1038/384270a0.
25. Krivega I, Dean A. 2016. Chromatin looping as a target for altering erythroid gene expression. Ann N Y Acad Sci 1368:31–39. https://doi.org/10.1111/nyas.13012.
26. Wadman IA, Osada H, Grutz GG, Agulnick AD, Westphal H, Forster A, Rabbitts TH. 1997. The LIM-only protein Lmo2 is a bridging molecule assembling an erythroid, DNA-binding complex which includes the TAL1, E47, GATA-1 and Ldb1/NLI proteins. EMBO J 16:3145–3157. https://doi.org/10.1093/emboj/16.11.3145.
27. Deng W, Lee J, Wang H, Miller J, Reik A, Gregory PD, Dean A, Blobel GA. 2012. Controlling long-range genomic interactions at a native locus by targeted tethering of a looping factor. Cell 149:1233–1244. https://doi.org/10.1016/j.cell.2012.03.051.
28. Krivega I, Dale RK, Dean A. 2014. Role of LDB1 in the transition from chromatin looping to transcription activation. Genes Dev 28:1278–1290. https://doi.org/10.1101/gad.239749.114.
29. Stadhouders R, Thongjuea S, Andrieu-Soler C, Palstra RJ, Bryne JC, van den Heuvel A, Stevens M, de Boer E, Kockx C, van der Sloot A, van den Hout M, van Ijcken W, Eick D, Lenhard B, Grosveld F, Soler E. 2012. Dynamic long-range chromatin interactions control Myb proto-oncogene transcription during erythroid development. EMBO J 31:986–999. https://doi.org/10.1038/emboj.2011.450.
30. Schuetzmann D, Walter C, van Riel B, Kruse S, Konig T, Erdmann T, Tonges A, Bindels E, Weilemann A, Gebhard C, Wethmar K, Perrod C, Minderjahn J, Rehli M, Delwel R, Lenz G, Groschel S, Dugas M, Rosenbauer F. 2018. Temporal autoregulation during human PU.1 locus Sub-TAD formation. Blood 132:2643–2655. https://doi.org/10.1182/blood-2018-02-834721.
31. Kraft S, Kinet JP. 2007. New developments in FcepsilonRI regulation, function and inhibition. Nat Rev Immunol 7:365–378. https://doi.org/10.1038/nri2072.
32. Ra C, Nunomura S, Okayama Y. 2012. Fine-tuning of mast cell activation by FcepsilonRIbeta chain. Front Immunol 3:112. https://doi.org/10.3389/fimmu.2012.00112.
33. Blank U, Ra CS, Kinet JP. 1991. Characterization of truncated alpha chain products from human, rat, and mouse high affinity receptor for immunoglobulin E. J Biol Chem 266:2639–2646.
34. Hiraoka S, Furumoto Y, Koseki H, Takagaki Y, Taniguchi M, Okumura K, Ra C. 1999. Fc receptor beta subunit is required for full activation of mast cells through Fc receptor engagement. Int Immunol 11:199–207. https://doi.org/10.1093/intimm/11.2.199.
35. Donnadieu E, Jouvin MH, Kinet JP. 2000. A second amplifier function for the allergy-associated Fc(epsilon)RI-beta subunit. Immunity 12:515–523. https://doi.org/10.1016/S1074-7613(00)80203-4.
36. Pino-Yanes M, Corrales A, Cumplido J, Poza P, Sánchez-Machín I, Sánchez-Palacios A, Figueroa J, Acosta-Fernández O, Buset N, García-Robaina JC, Hernández M, Villar J, Carrillo T, Flores C. 2013. Assessing the validity of asthma associations for eight candidate genes and age at diagnosis effects. PLoS One 8:e73157. https://doi.org/10.1371/journal.pone.0073157.
37. Amo G, García-Menaya J, Campo P, Cordobés C, Serón MCP, Ayuso P, Esguevillas G, Blanca M, Agúndez JAG, García-Martín E. 2016. A nonsynonymous FCER1B SNP is associated with risk of developing allergic rhinitis and with IgE levels. Sci Rep 6:19724. https://doi.org/10.1038/srep19724.
38. Amo G, Cornejo-García JA, García-Menaya JM, Cordobes C, Torres MJ, Esguevillas G, Mayorga C, Martinez C, Blanca-Lopez N, Canto G, Ramos A, Blanca M, Agúndez JAG, García-Martín E. 2016. FCERI and histamine metabolism gene variability in selective responders to NSAIDs. Front Pharmacol 7:353. https://doi.org/10.3389/fphar.2016.00353.
39. Pavón-Romero GF, Pérez-Rubio G, Ramírez-Jiménez F, Ambrocio-Ortiz E, Bañuelos-Ortiz E, Alvarado-Franco N, Xochipa-Ruiz KE, Hernández-Juárez E, Flores-García BA, Camarena ÁE, Terán LM, Falfán-Valencia R. 2018. MS4A2-rs573790 is associated with aspirin-exacerbated respiratory disease: replicative study using a candidate gene strategy. Front Genet 9:363. https://doi.org/10.3389/fgene.2018.00363.
40. Hiroyama T, Miharada K, Sudo K, Danjo I, Aoki N, Nakamura Y. 2008. Establishment of mouse embryonic stem cell-derived erythroid progenitor cell lines able to produce functional red blood cells. PLoS One 3:e1544. https://doi.org/10.1371/journal.pone.0001544.
41. Calero-Nieto FJ, Ng FS, Wilson NK, Hannah R, Moignard V, Leal-Cervantes AI, Jimenez-Madrid I, Diamanti E, Wernisch L, Göttgens B. 2014. Key regulators control distinct transcriptional programmes in blood progenitor and mast cells. EMBO J 33:1212–1226. https://doi.org/10.1002/embj.201386825.
42. Creyghton MP, Cheng AW, Welstead GG, Kooistra T, Carey BW, Steine EJ, Hanna J, Lodato MA, Frampton GM, Sharp PA, Boyer LA, Young RA, Jaenisch R. 2010. Histone H3K27ac separates active from poised enhancers and predicts developmental state. Proc Natl Acad Sci U S A 107:21931–21936. https://doi.org/10.1073/pnas.1016071107.
43. Rada-Iglesias A, Bajpai R, Swigut T, Brugmann SA, Flynn RA, Wysocka J. 2011. A unique chromatin signature uncovers early developmental enhancers in humans. Nature 470:279–283. https://doi.org/10.1038/nature09692.
44. Ohmori S, Takai J, Ishijima Y, Suzuki M, Moriguchi T, Philipsen S, Yamamoto M, Ohneda K. 2012. Regulation of GATA factor expression is distinct between erythroid and mast cell lineages. Mol Cell Biol 32:4742–4755. https://doi.org/10.1128/MCB.00718-12.
45. Dignam JD, Lebovitz RM, Roeder RG. 1983. Accurate transcription initiation by RNA polymerase II in a soluble extract from isolated mammalian

nuclei. Nucleic Acids Res 11:1475–1489. https://doi.org/10.1093/nar/11.5.1475.
46. Ran FA, Hsu PD, Wright J, Agarwala V, Scott DA, Zhang F. 2013. Genome engineering using the CRISPR-Cas9 system. Nat Protoc 8:2281–2308. https://doi.org/10.1038/nprot.2013.143.
47. Dekker J, Heard E. 2015. Structural and functional diversity of topologically associating domains. FEBS Lett 589:2877–2884. https://doi.org/10.1016/j.febslet.2015.08.044.
48. Nora EP, Lajoie BR, Schulz EG, Giorgetti L, Okamoto I, Servant N, Piolot T, van Berkum NL, Meisig J, Sedat J, Gribnau J, Barillot E, Bluthgen N, Dekker J, Heard E. 2012. Spatial partitioning of the regulatory landscape of the X-inactivation centre. Nature 485:381–385. https://doi.org/10.1038/nature11049.
49. Dixon JR, Selvaraj S, Yue F, Kim A, Li Y, Shen Y, Hu M, Liu JS, Ren B. 2012. Topological domains in mammalian genomes identified by analysis of chromatin interactions. Nature 485:376–380. https://doi.org/10.1038/nature11082.
50. Phillips-Cremins JE, Sauria ME, Sanyal A, Gerasimova TI, Lajoie BR, Bell JS, Ong CT, Hookway TA, Guo C, Sun Y, Bland MJ, Wagstaff W, Dalton S, McDevitt TC, Sen R, Dekker J, Taylor J, Corces VG. 2013. Architectural protein subclasses shape 3D organization of genomes during lineage commitment. Cell 153:1281–1295. https://doi.org/10.1016/j.cell.2013.04.053.
51. Catarino RR, Stark A. 2018. Assessing sufficiency and necessity of enhancer activities for gene expression and the mechanisms of transcription activation. Genes Dev 32:202–223. https://doi.org/10.1101/gad.310367.117.
52. Chen H, Du G, Song X, Li L. 2017. Non-coding transcripts from enhancers: new insights into enhancer activity and gene expression regulation. Genomics Proteomics Bioinformatics 15:201–207. https://doi.org/10.1016/j.gpb.2017.02.003.
53. Miyamoto T, Iwasaki H, Reizis B, Ye M, Graf T, Weissman IL, Akashi K. 2002. Myeloid or lymphoid promiscuity as a critical step in hematopoietic lineage commitment. Dev Cell 3:137–147. https://doi.org/10.1016/S1534-5807(02)00201-0.
54. Wontakal SN, Guo X, Smith C, MacCarthy T, Bresnick EH, Bergman A, Snyder MP, Weissman SM, Zheng D, Skoultchi AI. 2012. A core erythroid transcriptional network is repressed by a master regulator of myelo-lymphoid differentiation. Proc Natl Acad Sci U S A 109:3832–3837. https://doi.org/10.1073/pnas.1121019109.
55. May G, Soneji S, Tipping AJ, Teles J, McGowan SJ, Wu M, Guo Y, Fugazza C, Brown J, Karlsson G, Pina C, Olariu V, Taylor S, Tenen DG, Peterson C, Enver T. 2013. Dynamic analysis of gene expression and genome-wide transcription factor binding during lineage specification of multipotent progenitors. Cell Stem Cell 13:754–768. https://doi.org/10.1016/j.stem.2013.09.003.
56. Hoppe PS, Schwarzfischer M, Loeffler D, Kokkaliaris KD, Hilsenbeck O, Moritz N, Endele M, Filipczyk A, Gambardella A, Ahmed N, Etzrodt M, Coutu DL, Rieger MA, Marr C, Strasser MK, Schauberger B, Burtscher I, Ermakova O, Burger A, Lickert H, Nerlov C, Theis FJ, Schroeder T. 2016. Early myeloid lineage choice is not initiated by random PU.1 to GATA1 protein ratios. Nature 535:299–302. https://doi.org/10.1038/nature18320.
57. Strasser MK, Hoppe PS, Loeffler D, Kokkaliaris KD, Schroeder T, Theis FJ, Marr C. 2018. Lineage marker synchrony in hematopoietic genealogies refutes the PU.1/GATA1 toggle switch paradigm. Nat Commun 9:2697. https://doi.org/10.1038/s41467-018-05037-3.
58. Takahashi K, Nishiyama C, Hasegawa M, Akizawa Y, Ra C. 2003. Regulation of the human high affinity IgE receptor beta-chain gene expression via an intronic element. J Immunol 171:2478–2484. https://doi.org/10.4049/jimmunol.171.5.2478.
59. Takahashi K, Hayashi N, Kaminogawa S, Ra C. 2006. Molecular mechanisms for transcriptional regulation of human high-affinity IgE receptor beta-chain gene induced by GM-CSF. J Immunol 177:4605–4611. https://doi.org/10.4049/jimmunol.177.7.4605.
60. Iwasaki H, Somoza C, Shigematsu H, Duprez EA, Iwasaki-Arai J, Mizuno S, Arinobu Y, Geary K, Zhang P, Dayaram T, Fenyus ML, Elf S, Chan S, Kastner P, Huettner CS, Murray R, Tenen DG, Akashi K. 2005. Distinctive and indispensable roles of PU.1 in maintenance of hematopoietic stem cells and their differentiation. Blood 106:1590–1600. https://doi.org/10.1182/blood-2005-03-0860.
61. Charles MA, Saunders TL, Wood WM, Owens K, Parlow AF, Camper SA, Ridgway EC, Gordon DF. 2006. Pituitary-specific Gata2 knockout: effects on gonadotrope and thyrotrope function. Mol Endocrinol 20:1366–1377. https://doi.org/10.1210/me.2005-0378.